Magnetic Field Dependent Ordering in Ferrofluids at SiO_2 Interfaces

A. Vorobiev,[1,2] J. Major,[1] H. Dosch,[1,3] G. Gordeev,[2] and D. Orlova[2]

[1]*Max-Planck-Institut für Metallforschung, Heisenbergstr. 3, D-70569 Stuttgart, Germany*
[2]*Petersburg Nuclear Physics Institute RAS, 188300 Gatchina, St. Petersburg, Russia*
[3]*Institut für Theoretische und Angewandte Physik, Universität Stuttgart, Germany*

(Received 21 July 2004; published 21 December 2004)

We report pronounced smecticlike ordering in a ferrofluid adjacent to a SiO_2 wall. In the presence of small magnetic fields perpendicular to the interface, ordered layers of magnetite nanoparticles form that can extend up to 30 layers. We also show that short ranged ordered structures emerge when the magnetic field direction is parallel to the interface; however, the layering is strongly perturbed. These results have been obtained by *in situ* neutron reflectometry which gives a detailed microscopic picture of these ordering phenomena. They also reveal the formation of a wetting double-layer which forms the magnetic template for the observed ordering sheets. The implications of these findings are discussed.

DOI: 10.1103/PhysRevLett.93.267203 PACS numbers: 75.70.Cn, 61.12.Ha, 61.30.Hn, 75.50.Mm

Ferrofluids—also known as magnetic colloids—are textbook examples of a fluid material with properties tailored on the nanometer level. They consist of single-domain magnetic particles with a typical size of 10 nm dispersed in a liquid carrier [1,2]. Because of their superparamagnetic susceptibility, they can conveniently be manipulated by external magnetic fields which allows one to position and safely fix ferrofluid droplets in (micro-) mechanical devices as seals or heat dissipators, realized today in modern hard disc drives or in high power loudspeaker coils, respectively [3]. Ferrofluids are also known as magneto-rheological fluids since their viscosity depends sensitively upon external magnetic fields giving rise to their well-known non-Newtonian hydrodynamic behavior [4,5].

From a more fundamental perspective, the complex but well-controlled competing interactions make them scientifically very attractive examples of disordered materials: the strongly anisotropic dipole-dipole interaction between the nanoparticles leads to the prediction of a rich phase diagram and of spontaneous wormlike local correlations [6]. A strong steric repulsion, mostly introduced by coating the magnetic colloids with a thin polymer film consisting of a self-assembled mono- or double-layer of fatty acid radicals [see Fig. 1(a)], prevents coagulation of the nanoparticles and, assisted by Brownian motion, sedimentation under gravity. Finally, by applying external magnetic fields, the magnetic dipoles can be aligned, thereby enhancing their attractive interactions. Recent small-angle neutron scattering studies of ferrofluids in strong external magnetic fields revealed field-induced hexagonal ordering between the particles [7] as predicted by Monte Carlo simulations [8]. They are held responsible for the aforementioned field-dependent viscosity increase.

In this Letter we consider the effect of the ferrofluid-wall interactions onto ordering, an aspect which will become increasingly important in future nanoconfinement geometries. Experimental evidence of wall- or surface-induced ordering in ferrofluids is rather limited. A weak birefringence of polarized light has been observed at a glass-ferrofluid interface which is referred to the presence of ordered layers [9,10]. The strong off-specular x-ray scattering detected at a free ferrofluid surface has been explained by the presence of fractal chains of the magnetic particles [11]. Here we present a neutron reflectivity study of the ferrofluid structure at and close to a ferrofluid-SiO_2 interface as a function of small external magnetic fields, disclosing a detailed microscopic picture of the ordering phenomena. We will show *inter alia* that rather intriguing ordering structures develop which react sensitively upon the strength and direction of the applied field.

Dispersed Fe_3O_4 (''magnetite'') nanoparticles have been prepared by chemical deposition. Subsequent coating with a double-layer of $C_{18}H_{33}NaO_2$ surfactant molecules (''sodium oleate'') renders the nanoparticles hydrophilic and assures stability of the suspension [3]. Further details are described in Fig. 1(a). In the ferrofluid used for the neutron study, these magnetic particles have been dissolved with an Fe_3O_4 concentration of 9 vol. % in D_2O (''heavy water'').

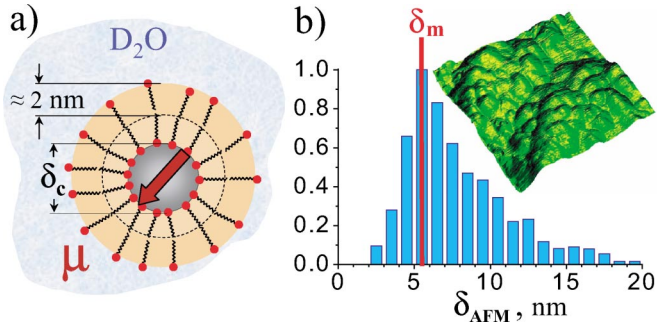

FIG. 1 (color). (a) Structure of the colloidal particle with the magnetite core of size δ_c and the sodium oleate double layer. The (hydrophilic) polar heads are shown as red dots. (b) AFM data and deduced size distribution of dried particles. $\delta_m = (5.5 \pm 0.5)$ nm is the maximum in the distribution.

In order to measure the size distribution, the ferrofluid has been sprayed on a Si substrate, then dried in air and characterized by atomic force microscopy (AFM) in the tapping mode using a Au-coated Si cantilever. A typical result is shown in Fig. 1(b) together with the deduced size distribution which shows a maximum at $\delta_m = (5.5 \pm 0.5)$ nm (note that this value gives the size distribution of the magnetic cores covered with a collapsed surfactant layer). The actual sample assembly (see Fig. 2) consists of the ferrofluid brought into contact with a highly polished Si surface covered with a 1.5 nm thick native SiO_2 layer. Its rms roughness is 0.5 nm as determined by neutron reflectometry.

The neutron reflectometry studies have been performed using the EVA reflectometer [12,13] at the High Flux Reactor in Grenoble in the vertical reflection mode with a neutron wavelength of $\lambda = 5.5$ Å. The collimated incident neutron beam k_i penetrates the Si substrate crystal and undergoes internal reflection at the ferrofluid-SiO_2 interface (Fig. 2). The exit-angle distribution $I(\alpha_f)$ of the scattering from the interface is recorded by a linear position sensitive detector [Fig. 2(a)] as function of the incidence angle α_i. The specular reflected intensity $I(q_z)$ [marked red in Fig. 2(a)] carries detailed information on the (scattering length) density profile $\rho(z)$ within the ferrofluid adjacent to the SiO_2 wall and thus gives direct access to any ordering phenomena perpendicular to the interface (q_z is the neutron momentum transfer perpendicular to the surface; for further information see, e.g., [14,15]). The experimental scheme and the profile reconstruction is shown schematically in Fig. 2: the recorded

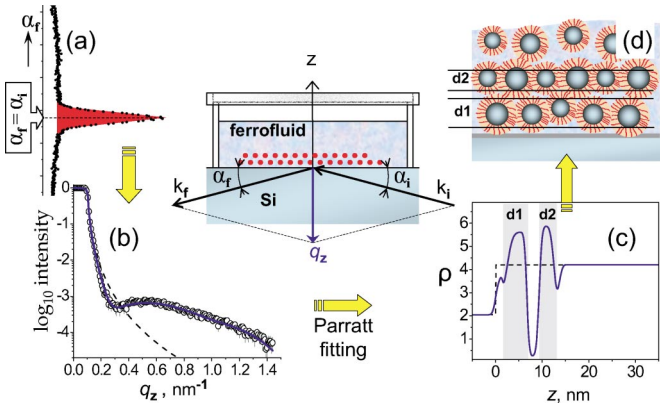

FIG. 2 (color). Scheme of the experimental setup, data recording, data treatment, and models. Center: sketch of the experiment showing the incident and reflected neutron beam (k_i, k_f) and the sample assembly. q_z is the momentum transfer perpendicular to the interface. (a) Example of a neutron spectrum as recorded by a position sensitive detector (the red area is the background-corrected reflected intensity). (b) Reflected intensity versus q_z. The blue line is a best fit; the dashed line shows the Fresnel curve (see main text). (c) (Scattering length) density profile $\rho(z)$ as deduced from (b) via a Parratt fitting algorithm. (d) Real space distribution of the nanoparticles deduced from (c).

intensity $I(q_z)$ [Fig. 2(b)] is background corrected and fitted to a model profile $\rho(z)$ [Fig. 2(c)] using the Parratt formalism [16]. The best density profile is determined by a least squares fit analysis and finally translated into a microscopic model [Fig. 2(d)].

In what follows, we describe our experimental findings as observed at around 30 °C. They will be subdivided into three groups: (a) the spontaneous formation of a nanoparticle double layer (''wetting layer''), (b) the development of an extended ordered sheet on top of this wetting layer in the presence of a weak magnetic field perpendicular to the interface ($H_\perp = 50$ Oe, 105 Oe), and (c) short ranged ordering effects in the presence of a magnetic field parallel to the interface ($H_\parallel = 105$ Oe).

(a) *Formation of a wetting layer.*—Figure 2(b) shows the neutron reflectivity curve recorded 24 hours after assembling the ferrofluid-SiO_2 interface. It shows a pronounced deviation from the Fresnel curve associated with a homogenous ferrofluid density [dashed line in Fig. 2(c)] adjacent to the interface. The best fit [blue line in Fig. 2(b)] is obtained by density profile composed out of two minima and two maxima at the interface [blue line in Fig. 2(c)] which are associated with the densities of the surfactant layer and the magnetite core of the colloidal nanoparticles, respectively. This is a clear evidence of the formation of a dense double layer of colloidal particles separated by a surfactant layer [Fig. 2(d)]. Interestingly, the first Fe_3O_4 layer is somewhat smeared out as disclosed by the reduced lateral density and a broader spacing $d_1 = (4.3 \pm 0.1)$ nm, while the second Fe_3O_4 layer is very well defined with an average spacing of $d_2 = (3.3 \pm 0.1)$ nm. A more detailed analysis of the experimental results shows that this double layer must form within 1 h and then remains stable.

(b) *Extended ordering sheet in the presence of $H_\perp$.*—For the experiments with external fields, a pair of Helmholtz coils has been mounted, assuring a homogeneity of the field over the sample area of better than 1%. Figure 3(a) shows the experimental observation after applying a field of $H_\perp = 50$ Oe: the reflectivity curve exhibits, in addition to the broad feature associated with the wetting layer discussed before, a second interference maximum at $q_z = 0.99$ nm^{-1}. The best fit (red line) gives clear evidence for an exponentially decaying ordering layer with a decay length of $\xi_z = 17$ nm on top of the wetting layer. Figure 3(b) shows the ordering phenomena after the magnetic field has been increased to $H_\perp = 105$ Oe: curve I is found 24 hours after the field change, curve II 48 hours afterwards. The intensity increase and the width decrease of the ''Bragg signal'' directly implies the formation of an extended ordering sheet consisting of approximately 15 colloidal layers followed by a exponentially decaying ordered skin with $\xi_z = 43$ nm (right side of Fig. 3). The clear shift of the Bragg maximum from $q_z = 1.01$ nm^{-1} to $q_z = 1.21$ nm^{-1} [arrow in Fig. 3(b)] during the growth of the ordered sheet points to a substantial densification of the

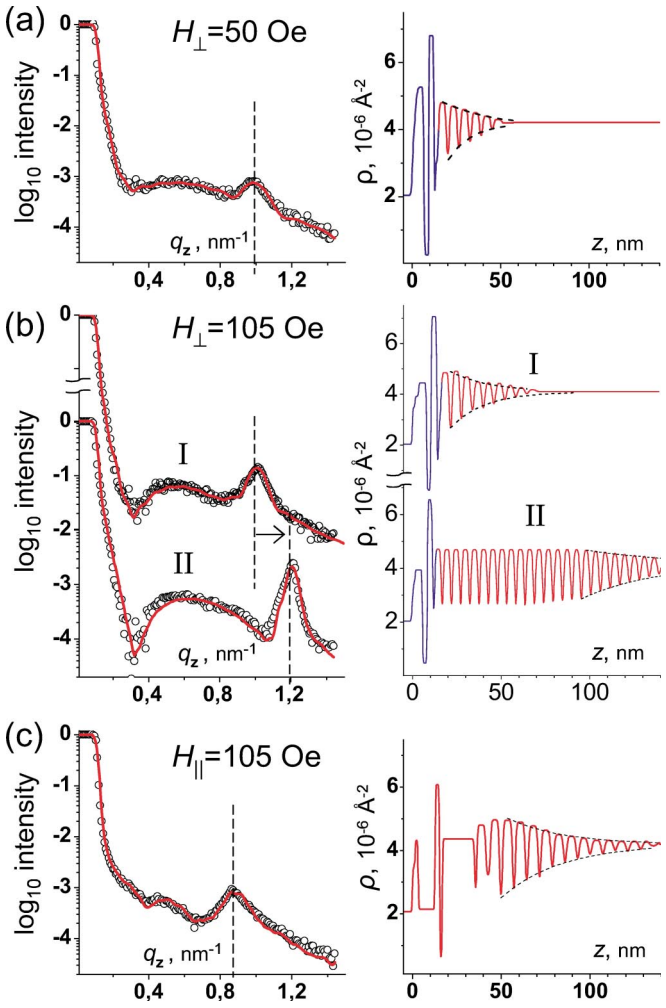

FIG. 3 (color). Experimental results (left) and deduced density profiles (right) for various experimental conditions. The red lines on the left show the best model from a least squares fit; the blue part of $\rho(z)$ denotes the wetting layer. (a) $H_\perp = 50$ Oe. (b) $H_\perp = 105$ Oe after 24 hours (curve I) and after 48 hours (curve II). (c) $H_\parallel = 105$ Oe. For the further explanations, see main text.

ordered layers; i.e., the normal interlayer distance decreases from $a_z = (2\pi)/q_z = 6.2$ nm to $a_z = 5.2$ nm. Apparently, the surfactant layers are squeezed together during ordering. The typical time scale for the formation of this ordered sheet is around 1 layer/hour.

(c) *Short ranged ordering effects in the presence of* $H_\parallel$.—When a parallel field is applied [Fig. 3(c)], we still observe ordering; however, with three distinctly different features which are quite remarkable: first, the Bragg maximum remains broad associated with a limited range of order perpendicular to the SiO_2 interface, as depicted on the right side of Fig. 3(c). Second, the Bragg maximum is shifted now to $q_z = 0.86$ nm^{-1} disclosing a significant expansion of the layered structure to $a_z = 7.3$ nm perpendicular to the interface. Third, we find a significant disorder in the layered structure. This shows that the parallel-field configuration gives also rise to ordering normal to the wall; however, the order is only short ranged and very strongly perturbed.

Table I summarizes our main observation, i.e., the number N of ordered layers, the lattice constant a_z of the layered structure, and the decay length ξ_z of the short ranged ordered regions.

In order to appreciate the role of the SiO_2 interface for these extended ordering phenomena, one must note that even in such concentrated ferrofluid as used here, both the Langevin ($\mu_0 m_p H/k_B T$) and magnetodipolar interaction ($\mu_0 m_p^2/4\pi r^3 k_B T$) parameters are of the order of 10^{-1} and thus too small to explain the observed ordering. (r is the particle-particle distance, $m_p = M_s V$ is the particle magnetic moment, M_s the saturation magnetization of magnetite, and V the particle volume). One may speculate that the decoration of the SiO_2 wall with the dense magnetic double layer creates an interface with a high magnetic susceptibility. When an external magnetic field is applied, the magnetic moments of the nanoparticles adjacent to this magnetic wall experience a preferential alignment parallel to the field. In turn, the attractive dipole-dipole interaction is enhanced along the field direction, while perpendicular to the field direction, the dipolar arrangement gives rise to a repulsive interaction. Thus, the perpendicular field configuration in our setup favors ordering normal to the interfaces and the observed compression of the surfactant layers; simultaneously it causes a separation of the nanoparticles within the layers. In the parallel-field configuration, ordering chains are favored parallel to the interface while they repel each other perpendicular to the interface, giving rise to the observed expansion and the disorder in the layering spacing.

In order to get an experimental clue on the lateral domain size of the ordered structures, we performed off-specular diffuse neutron scattering studies around the ordering Bragg signal at $q_z = 1.2$ nm^{-1}. Figure 4 shows $q_z - q_x$-scattering map as recorded for $H_\perp = 105$ Oe [associated with curve II in Fig. 3(b)]. The inplane intensity distribution (also shown in Fig. 4) exhibits an intrinsic (i.e., resolution corrected) width of $\Gamma_x = 2.3 \times 10^{-3}$ nm^{-1}. Interestingly, we find that the lateral domain size of the ordered structures increases slightly with field, but then saturates rather quickly with further field increase at a

TABLE I. Main fitting results from the reflectivity profiles shown in Fig. 3.

Condition	N	a_z [nm]	ξ_z [nm]
$H = 0$	0	...	...
$H_\perp = 50$ Oe	6	6.3 ± 0.1	17 ± 3
$H_\perp = 105$ Oe (I)	9	6.2 ± 0.1	21 ± 3
$H_\perp = 105$ Oe (II)	30	5.2 ± 0.1	43 ± 3
$H_\parallel = 105$ Oe	15	7.3 ± 0.1	33 ± 3

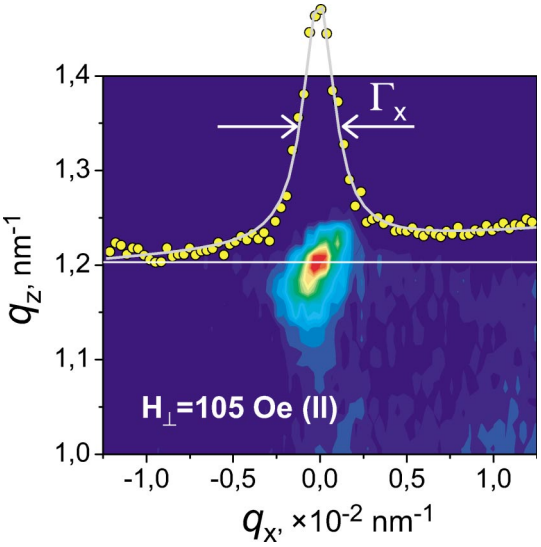

FIG. 4 (color). $q_z - q_x$ neutron scattering map around the ordering Bragg signal observed for $H_\perp = 105$ Oe. The yellow symbols show the intensity distribution parallel to the interface. Γ_x is the full width at half maximum.

value of $\ell_x = 2\pi/\Gamma_x = 3\ \mu$m. Thus, when the field is switched on, large flat ordered domains with a lateral extension of a few micrometers develop which then grow in height up to 200 nm.

In summary, we argue that the hydrophilic SiO_2 wall drives the formation of the ''wetting layer'' consisting of two very dense layers with a subsequent high magnetic response. All observed ordering phenomena are apparently mediated by the joint action of this high magnetic susceptibility of the wetting layer and the applied external fields. From our study, it appears that extended smecticlike order can be induced into ferrofluids at hard walls already in the presence of relatively moderate external magnetic fields. This must have ramifications when ferrofluids are used in nanoconfinement geometries because, according to our study, extended crystal-like structure can easily be frozen out close to interfaces. One may speculate, on the other hand, whether this very strong ordering tendency may be useful for a controlled growth of magnetically nanostructured interfaces eventually useful for data storage. Since the SiO_2 surface catalyzes smecticlike ordering of magnetic colloids so efficiently, SiO_2 lamellas may appear useful to enhance the magneto-rheological properties of ferrofluids.

We thank the ILL for continuous support and help and M. Jernenkov (JINR and ILL) for the AFM measurements. This work has been supported by the President of the Russian Federation (Grant No. NS-1671.2003.2) and the Russian State Program ''Neutron Research of Solids'' (MPN-Contract No. 40.012.1.1.1149) as well as by a focused neutron research funding of the Max Planck Society.

[1] R. E. Rosensweig, *Ferrohydrodynamics* (Cambridge University Press, Cambridge, England, 1985).
[2] E. Blums, A. Cebers, and M. M. Maiorov, *Magnetic Fluids* (de Gruyter, Berlin, 1997).
[3] B. M. Berkovsky, V. F. Medvedev, and M. S. Krakov, *Magnetic Fluids; Engineering Applications* (Oxford University Press, Oxford, 1993).
[4] M. I. Shliomis, Sov. Phys. Usp. **17**, 153 (1974).
[5] S. Odenbach, Int. J. Mod. Phys. **14**, 1615 (2000).
[6] P. G. de Gennes and P. A. Pincus, Phys. Kondens. Mater. **11**, 189 (1970); see also H. Pleiner, E. Jarkova, H.-W. Müller, and H. R. Brand, J. Magn. Magn. Mater. **252**, 147 (2002).
[7] A. Wiedenmann, A. Hoell, M. Kammel, and P. Boesecke, Phys. Rev. E **68**, 031203 (2003).
[8] S. Hess, J. B. Hayter, and R. Pynn, Mol. Phys. **53**, 1527 (1984).
[9] C. Y. Matuo, A. Bourdon, A. Bee, and A. M. Figueiredo Neto, Phys. Rev. E **56**, R1310 (1997).
[10] G. Barbero, A. Bourdon, A. Bee, and A. M. Figueiredo Neto, Phys. Lett. A **259**, 314 (1999).
[11] I. Takahashi, N. Tanaka, and S. Doi, J. Appl. Crystallogr. **36**, 244 (2003).
[12] H. Dosch, K. Al Usta, A. Lied, W. Drexel, and J. Peisl, Rev. Sci. Instrum. **63**, 5533 (1992).
[13] Evanescent-Wave Reflecto-Diffractometer EVA, http://www.ill.fr/YellowBook/EVA/
[14] G. P. Felcher, J. Appl. Phys. **87**, 5431 (2000).
[15] J. Als-Nielsen and D. McMorrow, *Elements of Modern X-Ray Physics* (Wiley, New York, 2001).
[16] L. G. Parratt, Phys. Rev. **95**, 359 (1954).